Effect of Ambient Pressure and Droplet Size on Droplet Vaporisation and Combustion

Shah Shahood Alam*, Ahtisham A. Nizami, Tariq Aziz

Abstract

In the present work, two cases of liquid droplet vaporisation and combustion were investigated with respect to high pressure and droplet size effects. Supercritical droplet vaporisation models for n-heptane-N_2 and LOX-H_2 systems were developed with considerations of high pressure liquid-vapour equilibrium, real gas effects and absorption of ambient gas in liquid layer at the droplet surface. A generalised code was developed using Newton-Raphson method. Appropriate relations were used for determining pressure dependent thermophysical and transport properties. It was observed that for n-heptane-nitrogen system, the critical mixing temperature increased with an increase in ambient pressure in the subcritical regime while decreased in the supercritical regime. Also, the solubility of nitrogen in liquid n-heptane increased with an increase in temperature in this regime. Further, at a given pressure, mass fraction of n-heptane vapour at the droplet surface increased with droplet temperature, while for a fixed droplet temperature, vapour mass fraction decreased with an increase in ambient pressure. For LOX-H_2 system, the critical mixing temperature increased progressively with pressure (unlike n-heptane-N_2 system) while hydrogen solubility in liquid oxygen increased with increasing temperature at supercritical pressures. Further, for a $100\,\mu m$ liquid oxygen droplet vaporising in hydrogen environment at $1000\,K$, evaporation lifetime for the droplet decreased for spherically symmetric case (gas phase Reynolds number $Re_g = 0$), as ambient pressure was increased from subcritical to supercritical value and further reduction in evaporation lifetime was noticed with an increase in Re_g. Also, for fixed values of ambient temperature and Re_g, maximum evaporation rate increased as ambient pressure was increased from 5.04 bar (reduced pressure P_r = 0.1) to 126 bar (P_r = 2.5).

Effect of initial droplet diameter was explored by developing a transient gas phase combustion model. It was observed that droplet burning was an unsteady event. Effect of droplet size on combustion characteristics showed that at a given pressure, droplet lifetime and burning rate increased. Further, for a wide range of droplet size ($20\,\mu m$ to $5000\,\mu m$), the flame diameter first increased, reached a maxima and then reduced to a minimum value at the end of droplet lifetime, so was the case with flame standoff distance.

Keywords: High pressure droplet vaporisation model, effects of supercritical vaporisation, unsteady gas phase model, numerical technique, effects of droplet size, different fuels, spray combustion.

*Corresponding author. E-mail: sshahood2004@yahoo.co.in. Address: Pollution and Combustion Engineering Lab. Department of Mechanical Engineering, Aligarh Muslim University, Aligarh-202002, U.P. India.

1 INTRODUCTION

1.1 Droplet Evaporation and Combustion at High Pressures

Droplet evaporation and combustion is prevalent in the spray combustion of liquid hydrocarbon fuels occuring in the combustion chambers of gas turbine and diesel engines, oil fired furnaces and liquid rockets and serves as the fundamental step for understanding the complex nature of spray burning.

Spherically symmetric assumption further leads to a simple geometry and one dimensional approach to the problem. It can be achieved in microgravity droplet combustion experiments. In some applications like diesel engines, liquid rockets and gas turbine engines, fuel droplets are subjected to temperatures and pressures beyond their critical point during the combustion process. This gives rise to a number of interesting phenomena at the critical point. Of particular importance in the study are the changes in the specific heat (c_p) of the fuel, which goes to infinity, and the latent heat of vaporisation which goes to zero at the critical point. Unresolved and controversial topics of interest include prediction of phase equilibrium at high and supercritical pressure including the choice of a proper equation of state. Influence of d^2-*law* behaviour at supercritical conditions, and the reduced surface tension.

High pressure and supercritical ambient conditions have a considerable influence on the mechanisms controlling engine behaviour and performance. Most of these effects are related to droplet behaviour. When liquid is injected into a combustion chamber that is filled with a gas at supercritical thermodynamic conditions, all aspects of the combustion process from atomisation to chemical reaction can be expected to depart significantly from the better known subcritical patterns. Studies in the past have investigated how and to what extent supercritical conditions may affect various aspects of the combustion of an isolated droplet in a quiescent environment.

In major industrial and space applications such as high output combustors for aircraft engines, liquid fueled rocket engines and diesel engines, manufacturers are looking for high pressure combustion systems for improving engine efficiency and power density. In fact, in recent years, diesel engine manufacturers have striven to increase the ambient chamber density and thereby pressure during fuel injection for achieving better mixing and increased rates of combustion. The operating pressure often exceeds the critical pressure of the liquid fuel. The droplets in the liquid fuel spray ignite and burn in the gaseous medium at temperatures and pressures above the thermodynamic critical state of the fuel.

The study of droplet behaviour in high pressure environment presents a scientifically challenging problem. The actual combustion process is characterised by the supercritical combustion of relatively dense sprays in highly convective environment. However, most studies considered decoupled problems in order to isolate a limited set of issues. Consequently, most results were derived in the case of an isolated droplet vaporising (no reactions) in a quiescent environment. Convective effects, influence of neighbouring droplets, detailed chemical kinetics or product condensation have received less and more recent attention [1].

Because high pressure tests are expensive and sometimes dangerous, considerable effort has been devoted to the development of accurate models capable of portraying the physics of drop evolution at high pressures. Predictions from such models, for example the validity of the d^2-*law* at high pressures, would enable a considerable simplification in the incorporation of drop models in the complex Computational Fluid Dynamics (CFD) codes [2].

Earlier research in this area included Spalding [3], who theoretically considered high pressure combustion by approximating the droplet vapour as an instantaneous point source of fuel. The combustion process was represented by a flame surface approximation, that is a diffusion flame with an infinitely thin reaction zone, constant properties were assumed, and convection was neglected. This analysis was modified by Rosner [4] to account for

the finite dimensions of the puff of gas. The influences of convection, density variation and finite rate chemical kinetics on supercritical combustion were studied by Brzustowski [5]. Manrique and Borman [6] found that effect of thermodynamic non idealities, property variations and high pressure corrections for phase equilibrium could influence the vaporisation mechanisms significantly.

Lazar and Faeth [7] and Canada and Faeth [8] conducted a series of experimental and theoretical studies on droplet combustion of hydrocarbon fuels in both stagnant and forced convective environments, with special attention focussed on high pressure phenomena of phase equilibrium. The effects of forced convection in the gas phase were treated by conventional multiplicative corrections.

Rosner and Chang [9] examined the effects of transient processes, natural convection, and the conditions under which a droplet may be driven to its critical point. Kadota and Hiroyasu [10] conducted an experimental study of combustion of suspended fuel droplets of n-heptane, n-decane, n-dodecane, n-hexadecane, iso-octane and light oil drops at reduced pressures as large as 1.5, and even 2.7 for oil under the influence of natural convection.

For all fuels, the final droplet temperature was nearly equal to its critical temperature and independent of ambient pressure in supercritical conditions. The combustion lifetime, defined as the time from the appearance of flame to its disappearance, displayed an abrupt reduction with P_r upto the critical point after which the reduction was only gradual, whereas the burning constant increased with an increase in pressure throughout subcritical and supercritical conditions.

Effects of ambient pressure and temperature on commercial multicomponent fuels like aviation gasoline, JP5 and diesel oil (DF2) were investigated by Chin and Lefebvre [11]. Their results suggested that evaporation constant k_{ev} values were enhanced as ambient pressure and temperature was increased.

Other research groups like Hsieh et al. [12], Curtis and Farell [13], Jia and Gogos [14] and Delplanque and Sirignano [15] employed numerical techniques to simulate high pressure droplet vaporisation and combustion with considerable success. Among them, Delplanque and Sirignano [15] developed an elaborate numerical model to investigate spherically symmetric, transient vaporisation of a liquid oxygen (LOX) droplet in quiescent, gaseous hydrogen at moderate and high pressures. Computations were performed for pure vaporisation of a $50\,\mu m$ LOX droplet initially at $100\,K$ at a reduced temperature T_r=9.70, and reduced pressures of P_r=2.0, 3.0 and 4.0.

They suggested that when film theory is used to model droplet combustion, the film surrounding the droplet can be assumed to be quasi-steady, since the characteristic time for heat diffusion through the film is typically two orders of magnitude smaller than the droplet lifetime. They advocated the use of Redlich-Kwong equation of state used by spray combustion community for its simplicity and accuracy for computing gas phase equilibrium mole fractions at high pressures. They further suggested that for a simplified droplet vaporisation model to be used in spray codes at supercritical conditions, it can be assumed that dissolved hydrogen remains confined in a thin layer at the droplet surface.

The effect of non equilibrium phase transition on droplet behaviour was further addressed by Harstad and Bellan [16-19] using Keizer's fluctuation theory. Umemura and Shimada [20] reported a numerical investigation of spherically symmetric droplet vaporisation under supercritical conditions. They identified the transition from subcritical to supercritical state in terms of a binary diffusion coefficient, which was suitably modified so that it became zero as the doplet surface reaches the critical mixing state.

Zhu and Aggarwal [21] carried out numerical investigation of supercritical vaporisation phenomena for n-heptane-N_2 system by considering transient, spherically symmetric conservation equations for both gas and liquid phases, pressure dependent thermophysical properties and detailed treatment of liquid-vapour phase equilibrium employing different equations of state. Yang [22] also analysed numerically a fully transient model

for LOX-H_2 system employing complex Benedict-Webb-Rubin EOS.

In another microgravity combustion study by Vieille et al.[23], high pressure droplet burning characteristics of five fuels (methanol, ethanol, n-hexane, n-heptane and n-octane) were investigated under normal and reduced gravity conditions using suspended droplet technique employing initial droplet diameters of about 1.5mm. An important result was that the d^2-*law* holds even under very high pressure and allows the estimation of an average droplet burning rate. The experimental results for all fuels showed that the droplet burning lifetime decreases strongly with increasing pressure in the subcritical regime.

Stengele et al.[24] conducted experimental and theoretical study, where the evaporation of free falling, non interacting, single and bicomponent droplets in a stagnant high pressure gas was investigated at different temperatures. Due to the relative velocity between the falling droplet and the stagnant gas, convective effects were incorporated through experimental correlations. The experimental results were compared with numerical calculations based on the conduction limit and diffusion limit model.

The effect of ambient pressure on the evaporation of a droplet and a spray of n-heptane was investigated by Kim and Sung [25] using a model for evaporation at high pressure. Their model considered phase equilibrium using the fugacities of liquid and gas phases for real gas behaviour and its importance on the calculation of the evaporation of the droplet or spray at high pressures was demonstrated. For the evaporation of single droplet, droplet lifetime increased with pressure at a low ambient temperature ($453\,K$) but decreased at high temperatures. The evaporation of a spray was enhanced by increasing the ambient pressure and the effect was more dominant at higher ambient temperatures.

From the literature review, it was felt that there was still a need of developing a high pressure droplet vaporisation model with considerations of high pressure liquid-vapour equilibrium, real gas effects, absorption of ambient gas in a thin layer at the droplet surface and pressure dependent properties which should be simple and realistic to be incorporated in spray analysis and tested for different systems. So that, the validity of d^2-*law*, surface temperature behaviour, solubility of ambient gas in the liquid and effects of convection could then be quantified.

1.2 Effect of Initial Droplet Diameter on Droplet Combustion Characteristics

Apart from ambient variables, initial droplet diameter plays an important role on droplet combustion characteristics. For example, the lifetime of the largest droplet in a spray determines the minimum time the droplet must be allowed to reside inside the combustion chamber.

Kumagai and co-workers [26,27,28] were pioneers in conducting spherically symmetric droplet combustion experiments in microgravity conditions through drop towers, capturing the flame movement and further showed that F/D ratio varies throughout the droplet burning history.

Waldman [29] and Ulzama and Specht [30] used analytical procedure whereas Puri and Libby [31] and King [32] employed numerical techniques in developing spherically symmetric droplet combustion models. The results of these authors were however mainly confined to the observations that unlike quasi-steady case, flame is not stationary and flame to droplet diameter ratio increases throughout the droplet burning period. The present work has tried to quantify the effect of initial droplet diameter on important combustion characteristics through a droplet combustion model.

2 PROBLEM FORMULATION

2.1 Development of Droplet Vaporisation Model at High Pressure

Combustion chambers of diesel engines, gas turbines and liquid rockets operate at supercritical conditions. To determine evaporation rates of liquid fuel sprays (made up of discrete droplets) at high pressures, a prior thermodynamic analysis is a must. Important assumptions employed in the present high pressure model are:

Droplet shape remains spherical, viscous dissipation effects are neglected, ambient gas gets dissolved in the droplet surface layer only, gas

phase behaves in a quasi-steady manner, radiation heat transport is neglected and Soret and Dufour effects are not considered.

At high pressures, vapour-liquid equilibria for each component can be expressed as:

$$f_1^{(v)} = f_1^{(l)}$$
$$T^{(v)} = T^{(l)} \qquad (1)$$
$$P^{(v)} = P^{(l)}$$

where, the superscripts *(v)* and *(l)* stand for vapour and liquid respectively.

f_i is the fugacity for component or species "i" and can be integrated through the following relation

$$R_u T \ln \frac{f_i}{x_i P} = \int_V^{\infty} [(\frac{\partial P}{\partial n_i})_{T,V,n_j} - \frac{R_u T}{V}]\, dV - R_u T \ln Z \qquad (2)$$

The above equation suggests that f_i can be determined by the properties of the constituent components, the concentrations in both phases and the temperature and pressure of the system. To compute the integral of the above equation, a real gas equation of state such as Redlich-Kwong equation of state was chosen. The cubic equations and their constants are provided in (Table 1). They can be expressed in general form by the relation [33]:

$$P = \frac{R_u T}{v - b} - \frac{a}{v^2 + ubv + \omega b^2}$$

R_u is Universal gas constant

v is molar volume

T is absolute temperature (K)

ω is Pitzer's acentric factor

Equation (2) is then integrated. After simplification we get equation (3) which is given as:

$$\ln f_i = \ln x_i + \ln P + \frac{b_i}{b}(Z-1) - \ln(Z-B) - \frac{A}{B}\left[\frac{2\sum_{j=1}^{N} x_j a_{ij}}{a} - \frac{b_i}{b}\right] \ln\left(1+\frac{B}{Z}\right)$$

This equation is valid for both vapour and liquid phases. The dimensionless parameters A and B are defined as:

$$A = \frac{aP}{R_u^2 T^2} \qquad \text{and} \qquad B = \frac{bP}{R_u T} \qquad (4)$$

Redlich-Kwong equation can be written in the form of compressibility factor as:

$$Z^3 - Z^2 + \left(A - B - B^2\right) Z - AB = 0 \qquad (5)$$

The mixture compressibility factor "Z" can be determined using Cardan's method, where highest value of Z corresponds to vapour phase and the smallest value to liquid phase.

Rewriting equation (3) for components 1 and 2 respectively, we have,

$$\ln f_1 = \ln x_1 + \ln P + \frac{b_1}{b}(Z-1) - \ln(Z-B) - \frac{A}{B}\left[\frac{2}{a}\left(x_1 a_{11} + x_2 a_{12}\right) - \frac{b_1}{b}\right] \ln\left(1+\frac{B}{Z}\right) \qquad (6)$$

$$\ln f_2 = \ln x_2 + \ln P + \frac{b_2}{b}(Z-1) - \ln(Z-B) - \frac{A}{B}\left[\frac{2}{a}\left(x_1 a_{21} + x_2 a_{22}\right) - \frac{b_2}{b}\right] \ln\left(1+\frac{B}{Z}\right) \qquad (7)$$

The parameters a and b in the cubic equation can be expressed in terms of composition and pure components parameters

$$a = \sum_{i=1}^{2}\sum_{j=1}^{2} x_i x_j a_{ij}\,, \qquad b = \sum_{i=1}^{2} x_i b_i \qquad (8)$$

The constants a_{ij} and b_i are essentially dependent on the critical properties of each species. In addition, proper mixing rules have to be employed to determine various mixing parameters for different mixtures.

The mixture constants *a* and *b* and subsequently dimensionless parameters *A* and *B* can be evaluated by substituting the assumed values of the mole fractions of the two components. Now since equation (3) can be applied to both vapour and liquid phases, if we have a two component, two phase system in equilibrium at a given temperature and pressure then there are four mole fractions $x_1^{(v)}$, $x_2^{(v)}$, $x_1^{(l)}$ and $x_2^{(l)}$ as unknowns for the phase equilibrium system. These unknowns have to be solved from four separate equations.

Therefore, equation (3) can be written for liquid and vapour phases for component "1" (equation 6). Then since at equilibrium, $f_1^{(l)} = f_1^{(v)}$, we get a relationship between $x_1^{(v)}$ and $x_1^{(l)}$. In the same manner, using equation (7) for component "2", we get a relationship between $x_2^{(v)}$ and $x_2^{(l)}$ from the fact that $f_2^{(l)} = f_2^{(v)}$ at equilibrium,

further, in a mixture, $x_1^{(l)} + x_2^{(l)} = 1$ and $x_1^{(v)} + x_2^{(v)} = 1$, hence the four unknowns can be determined.

The solution procedure requires evaluation of two lengthy, non linear equations which need to be solved iteratively. In the present work, Newton-Raphson method has been used. The solution is obtained in the form of a diagram representing vapour-liquid phase equilibrium compositions for a particular system at various pressures.

For a spherically symmetric Oxygen fuel droplet vaporising in a stagnant high pressure H_2 environment in a (LOX-H_2 system), mass fraction of the fuel vapour (oxygen) at the droplet surface is given as:

$$y_{O_2}^v = x_{O_2}^v \times \frac{W_F}{W_t} \tag{9}$$

where,

W_t (total molecular weight) $= x_{O_2}^v \times W_{O_2} + x_{H_2}^v \times W_{H_2}$

Here, x^v (mole fraction of vapour phase) of both the components are determined from the computer programme. The same equation can be used for n-heptane-N_2 system.

The heat transfer number B_T for subcritical pressures is given as:

$$B_T = \frac{C_{pg}\left(T_\infty - T_b\right)}{L + C_{pl}\left(T_b - T_{lo}\right)} \tag{10}$$

where, T_{lo} is the initial droplet temperature,

HV or *L* is the latent heat of vaporisation and for subcritical pressures given as:

$$HV_{O_2} = HV_{1O_2}\left(\frac{1-T_{r_2}}{1-T_{r_1}}\right)^{0.38} \tag{11}$$

where, HV_1 is at normal boiling point ; $T_r = T_b / T_c$.

Equation (11) can also be used for n-heptane-N_2 system.

For supercritical pressures, B_T for LOX-H_2 system can be taken as [34]:

$$B_T = \frac{T_\infty - T_c'}{T_c' - T_{l_o}} \tag{12}$$

where, T_c' is the critical mixing temperature.

Mass evaporation rate m_{ev} for spherical droplet is

$$m_{ev} = 2\pi D \frac{\lambda_{g_{mix}}}{C_{pg_{mix}}} \ln(1 + B_T) \tag{13}$$

Droplet evaporation lifetime, t_{ev} is

$$t_{ev} = \frac{\rho_{l_{mix}} D_0^2}{8\left(\lambda_{g_{mix}} / C_{pg_{mix}}\right)\ln\left(1 + B_T\right)} \tag{14}$$

Instantaneous droplet radius can be determined from

$$\frac{dr_l}{dt} = -\frac{\lambda_{g_{mix}}}{\rho_{l_{mix}} C_{pg_{mix}} r_l}\ln\left(1 + B_T\right) \tag{15}$$

Proper determination of thermophysical and transport properties are essential specially for multicomponent, high pressure, high temperature studies since simulation results depend heavily upon the correct evaluation of properties. For the present work, it was observed that in general the error lies within 10% of the experimental values.

2.2 Development of Spherically Symmetric, Unsteady Droplet Combustion Model for the Gas Phase

Important assumptions invoked in the development of spherically symmetric gas phase droplet combustion model of the present study

Spherical liquid fuel droplet is made up of single chemical species and is assumed to be at its boiling point temperature surrounded by a spherically symmetric flame, in a quiescent, infinite oxidising medium with phase equilibrium at the liquid-vapour interface expressed by the Clausius-Clapeyron equation.

Droplet processes are diffusion controlled (ordinary diffusion is considered, thermal and pressure diffusion effects are neglected). Fuel and oxidiser react instantaneously in stoichiometric proportions at the flame. Chemical kinetics is infinitely fast resulting in flame being represented as an infinitesimally thin sheet.

Ambient pressure is subcritical and uniform. Conduction is the only mode of heat transport, radiation heat transfer is neglected. Soret and Dufour effects are absent.

Thermo physical and transport properties are evaluated as a function of pressure, temperature and composition. Ideal gas behaviour is assumed. Enthalpy 'h' is a function of temperature only. The product of density and diffusivity is taken as constant. Gas phase Lewis number Le_g is assumed as unity.

The overall mass conservation and species conservation equations are given respectively as:

$$\frac{\partial \rho}{\partial t}+\frac{1}{r^2}\frac{\partial}{\partial r}\left(r^2 \rho v_r\right)=0 \qquad (16)$$

$$\frac{\partial(\rho Y)}{\partial t}+\frac{1}{r^2}\frac{\partial}{\partial r} r^2\left[\rho v_r Y-\rho D\frac{\partial Y}{\partial r}\right]=0 \qquad (17)$$

Where;

t is the instantaneous time

r is the radial distance from the droplet center

ρ is the density

v_r is the radial velocity of the fuel vapour

D is the mass diffusivity

Y is the mass fraction of the species

equations (16) and (17) are combined to give species concentration or species diffusion equation for the gas phase as follows

$$\frac{\partial Y}{\partial t}=D_g\frac{\partial^2 Y}{\partial r^2}+\frac{2D_g}{r}\frac{\partial Y}{\partial r}-v_r\left(\frac{\partial Y}{\partial r}\right) \qquad (18)$$

D_g is the gas phase mass diffusivity

The relation for energy conservation can be written in the following form

$$\frac{\partial(\rho h)}{\partial t}+\frac{1}{r^2}\frac{\partial}{\partial r}\left[r^2\rho\left(v_r\cdot h-D.\,C_p\frac{\partial T}{\partial r}\right)\right]=0 \qquad (19)$$

The energy or heat diffusion equation for the gas phase, equation (20) can be derived with the help of overall mass conservation equation (16) and equation (19), as:

$$\frac{\partial T}{\partial t}=\alpha_g\frac{\partial^2 T}{\partial r^2}+\frac{2\alpha_g}{r}\frac{\partial T}{\partial r}-v_r\left(\frac{\partial T}{\partial r}\right) \qquad (20)$$

T is the temperature, α_g is gas phase thermal diffusivity. Neglecting radial velocity of fuel vapour v_r for the present model, equations (18) and (20) reduce to a set of linear, second order partial differential equations (eqns 21 and 22).

$$\frac{\partial Y}{\partial t}=D_g\frac{\partial^2 Y}{\partial r^2}+\frac{2D_g}{r}\frac{\partial Y}{\partial r} \qquad (21)$$

$$\frac{\partial T}{\partial t}=\alpha_g\frac{\partial^2 T}{\partial r^2}+\frac{2\alpha_g}{r}\frac{\partial T}{\partial r} \qquad (22)$$

The solution of these equations provide the species concentration profiles (fuel vapour and oxidiser) and temperature profile for the inflame and post flame zones.

The boundary and initial conditions based on this combustion model are as follows

$$at\ r=r_f;\ T=T_f,\ Y_{o,f}=0,\ Y_{F,f}=0$$

$$at\ r=r_\infty;\ T=T_\infty,\ Y_{o,\infty}=0.232,$$

$$at\ t=0;\ r=r_{lo},\ T=T_b,\ Y_{F,S}=1.0$$

where $r_l=r_{lo}\left(1-t/t_d\right)^{1/2}$ for $\left(0\le t\le t_d\right)$,

is the moving boundary condition coming out from the d^2-*law* (since droplet is at its boiling point temperature). Here, T_f and T_∞ are temperatures at the flame and ambient atmosphere respectively. $Y_{F,S}$ and $Y_{F,f}$ are fuel mass fractions respectively at the droplet surface and flame. $Y_{o,\infty}$ and $Y_{o,f}$ are oxidiser concentrations in the ambience and at the flame respectively, t is the instantaneous time, t_d is the combustion lifetime of the droplet, r_{lo} is the original or initial droplet radius and r_l is the instantaneous droplet radius at time "t".

The location where the maximum temperature $T=T_f$ or the corresponding concentrations $Y_{F,f}=0$ and $Y_{o,f}=0$ occur, was taken as the flame radius r_f. Instantaneous time "t" was obtained from the computer results whereas the combustion lifetime "t_d" was determined from the relationship coming out from the d^2-*law*. Other parameters like instantaneous flame to droplet diameter ratio (F/D), flame standoff

distance $(F\text{-}D)/2$, dimensionless flame diameter (F/D_0) etc, were then calculated as a function of time

Solution technique

Equations (21) and (22) were solved numerically using the "finite difference technique". The approach is simple, fairly accurate and numerically efficient [35]. Here the mesh size in radial direction was chosen as h and in time direction as k. Using finite difference approximations, equations (21) and (22) were descritised employing three point central difference expressions for second and first space derivatives, and the time derivative was approximated by a forward difference approximation resulting in a two level, explicit scheme (eqn 23) which was implemented on a computer.

$$T_m^{n+1} = \alpha\lambda_1(1-p_m)T_{m-1}^n + (1-2\alpha\lambda_1)T_m^n + \alpha\lambda_1(1+p_m)T_{m+1}^n \quad (23)$$

Here, $\lambda_1(mesh\ ratio) = k/h^2$, $p_m = h/r_m$,

$r_m = r_{lo} + mh$, $Nh = r_\infty - r_{lo}$, $m = 0,1,2....N$.

The solution scheme is stable as long as the stability condition $\lambda_1 < 1/2$ is satisfied.

3 RESULTS AND DISCUSSION

3.1 Effect of Ambient Pressure on Burning Constant, Droplet Lifetime, Mass Burning Rate and F/D Ratio

Burning constant

The burning constant k_b, a primary factor for characterising burning droplets has been verified experimentally. The variation of burning constant with increase in reduced pressure P_r is shown in Fig 1. The results of present study were compared with experimental results of Kadota and Hiroyasu [10] who conducted an experimental study of combustion of single suspended droplets in supercritical gaseous environments under the influence of natural convection. The trend of the two results is the same which suggests that k_b increases with an increase in ambient pressure.

The slight difference (approximately 15%) in the variation of k_b with P_r for both the studies may be due to the difference in the values of thermophysical and transport properties for the present study which were subsequently used to calculate combustion parameters such as B_T, k_b and t_d given in the form of correlations. (In the present work, adiabatic flame temperature was calculated first by Gülder's method [36]. Various properties were then determined by using property estimation techniques [33] at an average temperature of T_b and T_f for the inner zone and T_f and T_∞ for the outer zone). Another reason may be the presence of natural convection in the experimental investigation of [10] which resulted in slightly higher values of k_b, and lower values of t_d (Fig 2) at each P_r.

The same trend was also observed in the results of Nomura et al.[37] who considered spherically symmetric n-heptane droplet evaporating in a high pressure (upto 20 atmospheres) nitrogen ambience. Here, the droplet size was varied between 0.6 to 0.8 mm and ambient nitrogen temperature varied between $400\,K$ to $800\,K$. Their results suggested that as ambient pressure was increased, corresponding values of k_{ev} were increased at each pressure, as the temperature was raised from $400\,K$ to $800\,K$.

Droplet lifetime

Combustion lifetime (time from establishment of flame till the burnout of the droplet) or simply droplet lifetime is a critical parameter of importance in the design of combustion chambers. It is also related to other design parameters such as spray injection velocity, combustion geometry etc. Results of the present study were compared with those of Kadota and Hiroyasu [10] in Fig 2. Here values of combustion lifetime of droplet t_d are plotted against reduced pressure P_r. The results of both studies indicate that t_d decreases with an increase in the value of ambient pressure P_∞.

This trend is also consistent with the investigations of other workers like Faeth et al.[38], who conducted supercritical droplet combustion experiments in near zero gravity conditions in a freely falling apparatus with n-decane droplets having initial diameters in the range of 800 μm to 1000 μm. The gas environment consisted of various mixtures of nitrogen and oxygen initially at room temperature. The pressure range of the experiments was 100-2000 psia. Similar trends in the variation of t_d with P_∞ were observed by Kim and Sung [25] who modelled the evaporation of n-heptane droplet injected into gaseous nitrogen at high pressures (upto 50 atmospheres). The ambient temperatures taken were 600 K and 1200 K and initial droplet diameter was 0.5 mm. Their results also showed that at high ambient temperatures, t_{ev} decreased with increase in ambient pressure.

The same behaviour was also observed from the results of Jia and Gogos [39], who modelled the evaporation of spherically symmetric high pressure evaporation of n-hexane droplet in nitrogen environment. D_0 was taken as 100 μm, P_∞ varied between (1-100 atmospheres), T_∞ between (1000-2000 K).

Mass burning rate

This result (Fig 3) can be interpreted using $m_f = \pi r_l \rho_l k_b / 2$ (equation 24), i.e. if ambient pressure P_∞ is increased, then the cumulative effects of ρ_l and k_b for a fixed droplet radius r_l lead to an increase in the mass burning rate.

F/D ratio against reduced pressure at t/t_d =0

Effect of ambient pressure on F/D ratio is shown in Fig 4. It was observed that as reduced pressure values increase, there was a corresponding increase in F/D ratio at a particular time, t/t_d =0. The reason is that as ambient pressure is increased, boiling point of fuel is increased which leads to an increase in flame diameter F obtained from computed results. Then as droplet radius r_l is decreasing continuously, the ratio F/D increases as a function of P_r. The same trend was observed in the results of Kotake and Okazaki [40].

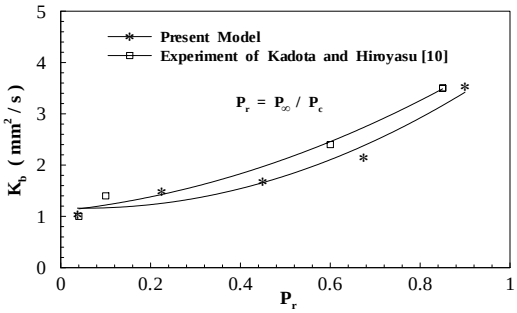

Figure 1: Effect of ambient pressure P_∞ on burning constant k_b for n - heptane (D_0 = 2000 microns, T_∞ = 298 K, $Y_{o,\infty}$ = 0.232)

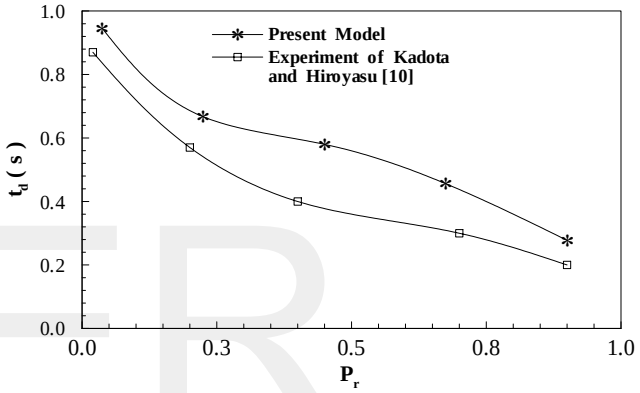

Figure 2: Ambient pressure effect on droplet lifetime

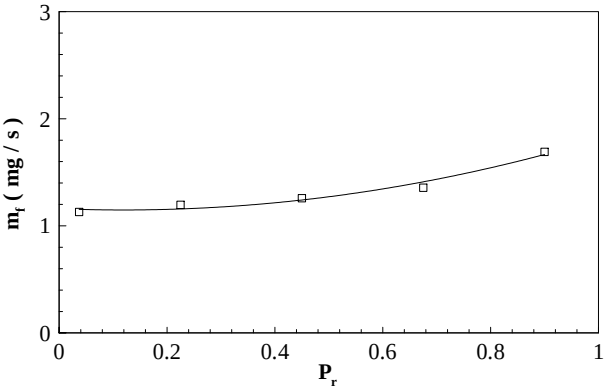

Figure 3 : Mass burning rate

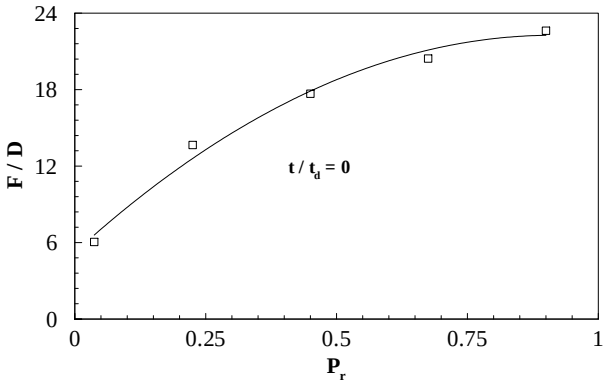

Figure 4: F / D ratio

3.2 Mole Fraction of n-Heptane Predicted by Redlich-kwong Equation of State for n-Heptane-Nitrogen System in Equilibrium at Sub and Supercritical Pressures

The variation of n-heptane mole fractions in liquid and vapour phases with temperature, when ambient pressure P_∞ is 13.7 bar (reduced pressure; P_r =0.5) is shown in Fig 5. This variation is also obtained for P_∞ =24.66 bar (P_r = 0.9) and for supercritical pressure P_∞ =68.5 bar (P_r =2.5) shown in Fig 6. The critical temperature and pressure for nitrogen are; T_c =126.2 K, P_c =33.9 bar and for n-heptane; T_c =540.3 K , P_c = 27.4 bar respectively. The critical mixing point obtained by employing Redlich-Kwong equation of state in the present work is the highest point of the curve where enthalpy of vaporisation goes to zero and there is no well defined interfacial boundary separating the liquid phase (n-heptane) from ambient gas (nitrogen).

It was observed that in the sub-critical regime the critical mixing temperature increases from 480K for P_r =0.5 to 530.1K for P_r =0.9 and then in supercritical region (P_r =2.5) decreases to 520K. This trend regarding the behaviour of critical mixing temperature is in good agreement with the simulation results of Zhu and Aggarwal [21], who developed a comprehensive, transient supercritical droplet vaporisation model by numerically solving conservation equations in liquid and gas phases using pressure dependent variable thermophysical properties and detailed treatment of liquid-vapour phase equilibrium employing different equations of state as compared to the simpler approach adopted in the present study. The small difference may be due to the methods employed for the evaluation of properties.

Another important observation is that in the subcritical regime, the amount of nitrogen dissolved in the liquid fuel (n-heptane) is very small at 300K, decreasing progressively with increasing temperature and reducing to zero at the critical mixing point. In supercritical pressure regime (P_r = 2.5), shown in Fig 6, it was observed that the solubility of nitrogen in the liquid n-heptane became progressively higher as the temperature was increased and becomes equal to about 0.3 at the critical mixing state.

The amount of nitrogen dissolved in n-heptane increased as the pressure was increased further, above P_r =2.5. Therefore, at appreciably high pressures, the amount of nitrogen dissolved in n-heptane may be quite significant and may modify the liquid properties and subsequently the vaporisation behaviour. Hence it is felt that supercritical modelling studies should include liquid phase solubility of gases.

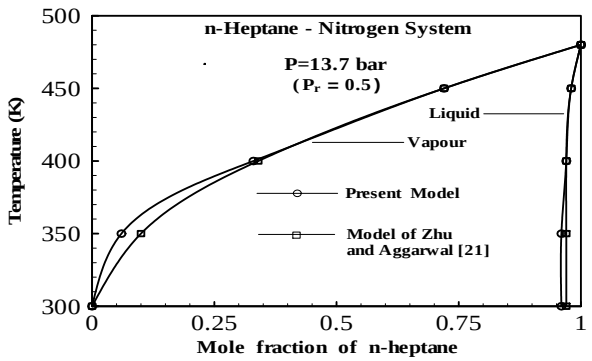

Figure 5 : Vapour-liquid phase equilibrium compositions predicted by Redlich-Kwong EOS for n-heptane-nitrogen system

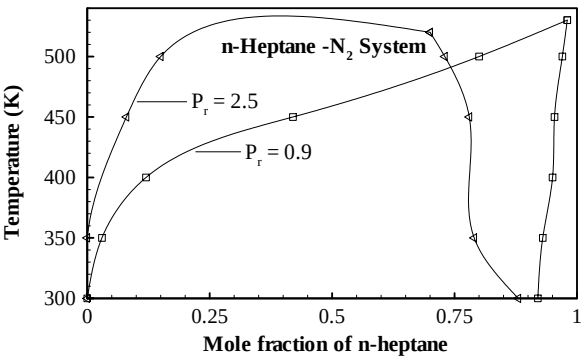

Figure 6: Vapour-liquid phase equilibrium compositions at subcritical and supercritical pressures

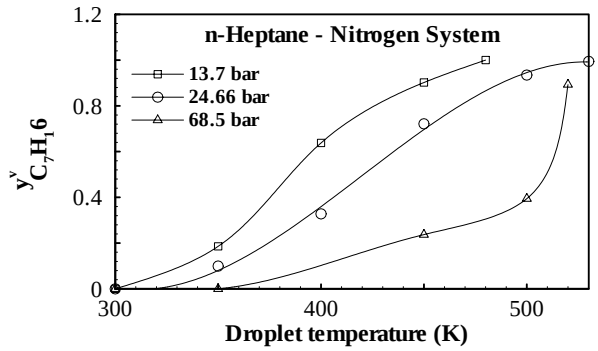

Figure 7: n-Heptane vapour mass fraction variation with droplet temperature at different pressures

3.3 Variation of n-Heptane Vapour Mass Fraction at the Droplet Surface with Droplet Temperature

Figure 7 shows the variation of n-heptane vapour mass fraction $y^{v}_{C_7H_{16}}$ with droplet surface temperature at three different pressures. The mole fractions of n-heptane vapour $x^{v}_{C_7H_{16}}$ were computed from the computer programme at each temperature and the corresponding vapour mass fractions $y^{v}_{C_7H_{16}}$ were determined using equation 9. For each pressure, mass fraction increased with an increase in droplet temperature and at a given temperature, mass fraction decreased with increasing pressure. The maximum values being 1.0 for subcritical and 0.9 for supercritical pressures respectively. Also at supercritical pressure of 68.5 bar, the mass fraction variation was small about 0.42 till 500*K*, but increased suddenly at a slight increase in temperature to a value of about 0.9 at 520*K*. A reason for this difference in behaviour may be due to the absorption of ambient nitrogen in liquid heptane droplet that could modify the droplet vaporisation characteristics.

3.4 Mole Fraction of Oxygen Predicted by Redlich-Kwong Equation of State for LOX–H_2 System in Equilibrium at Different Pressures

Figure 8 suggests that the critical mixing temperature increases progressively with an increase in pressure from 110 K at P_r=0.1 to 132 K at P_r=0.4 and 138.0 K at P_r=2.5 which is true for both the present results as well as those of Yang [22] who employed a detailed, fully transient numerical model with the complex eight constant Benedict-Webb-Rubin EOS, as compared to the present study which is simpler and accurate. It is further observed that in subcritical regime (P_r =0.1 to P_r=0.4), the amount of hydrogen dissolved in liquid oxygen was very small, decreasing progressively with increasing temperature and reducing to zero at the critical mixing temperature. However, at the supercritical pressure P_r=2.5, hydrogen solubility in liquid oxygen increased sharply with increasing temperature, being approximately equal to 0.4 for the present model.

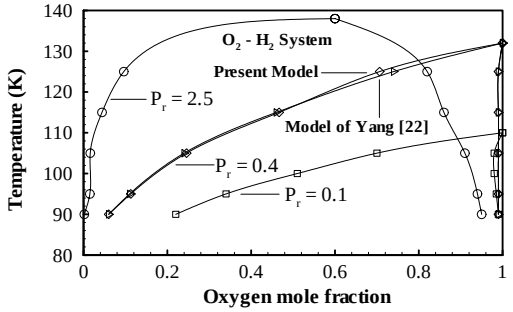

Figure 8 : Vapour-liquid phase equilibrium compositions for O_2/H_2 system at sub and supercritical pressures

3.5 Oxygen Vapour Mass Fraction Variation at the Droplet Surface with Droplet Temperature

Figure 9 shows the variation of oxygen vapour mass fraction $y_{o_2}^v$ with droplet surface temperature at different pressures. At each pressure, vapour mole fractions of oxygen $x_{o_2}^v$ were determined from the computed results as a function of temperature. The corresponding oxygen mass fraction $y_{o_2}^v$ were then calculated using equation 9.

For each pressure, mass fraction increased with droplet temperature. Further at a fixed droplet temperature, mass fraction decreased as pressure was increased. Also, unlike n-heptane-N_2 system, the initial mass fraction present at the droplet surface was 0.8 which decreased progressively with increase in pressure to a minimum value. For the supercritical pressure of 126 bar, there was a steep rise in the value of mass fraction with droplet surface temperature as compared to. P_r =0.1 and 0.4 cases. It was also noted that the maximum value of mass fraction was 0.959 for 126 bar whereas for subcritical pressures, maximum $y_{o_2}^v$ value was 1.0, emphasising the change in vaporising characteristics at very high pressures.

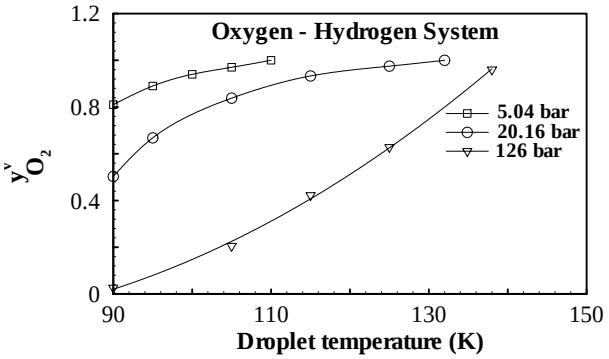

Figure 9: Oxygen vapour mass fraction variation with droplet temperature at various pressures

3.6 Square of Dimensionless Droplet Diameter $(D/D_0)^2$ Versus Time

The plot of $(D/D_0)^2$ (also called square of dimensionless surface area) with time for a hundred micrometer diameter oxygen droplet vaporising in hydrogen environment at a fixed ambient temperature of $1000\,K$ and $Re_g = 100$ is shown in Fig 10.

The procedure for getting the variation of instantaneous droplet radius r_l and subsequently $(D/D_0)^2$ with time was achieved by calculating high pressure specific heat $C_{pg_{mix}}$ and thermal conductivity $\lambda_{g_{mix}}$ of the gaseous mixture at T_∞ = $1000\,K$. Lee-Kesler method [33] was used to determine $C_{pg_{mix}}$ at high pressure and temperature together with Lee-Kesler mixing rules. Low pressure gas thermal conductivity was calculated first for pure components using Stiel and Thodos relation and for low pressure mixtures using Wassiljewa Equation, then using mixing rules suggested by Yorizane et al.[33], high pressure inverse gaseous mixture thermal conductivity was determined by Roy and Thodos formula and finally $\lambda_{g_{mix}}$ at high pressure was obtained using appropriate relation with respect to reduced mixture density ρ_{r_m}.

For high pressure liquid mixture densitiy $\rho_{l_{mix}}$, Hankinson and Thomson method was employed at low pressures, with high pressure correction provided by the modified Hankinson-Brobst-Thomson relation. Boiling point T_b and latent heat of vaporisation L were determined using a particular EOS and equation 11 respectively. Specific heat of liquid mixture at high pressure $C_{p_{lmix}}$ was evaluated from Rowlinson method. The heat transfer number B_T was calculated using equation 10 and droplet evaporation lifetime t_{ev} followed from equation 14. Finally the relationship between instantaneous droplet radius r_l with time was obtained by integrating equation 15. For supercritical pressure of 126 bar, B_T was calculated using equation 12.

For this forced convection case, the expression for droplet evaporation lifetime was modified [41] by incorporating the term (1+ $0.3\,Re_g^{0.5} \times Pr_g^{0.33}$). Pr_g was taken as unity since quasi-steady gas phase. Equation 15 was used for

getting the variation of r_l with time and subsequently $(D/D_0)^2$ with time for three different pressures corresponding to P_r = 0.1, 0.4, 2.5. This result represents a plot of $(D/D_0)^2$ versus time for practical systems where Re_g is of the order of 100 [1].

The results suggests that as ambient pressure is increased for a fixed value of ambient temperature, the evaporation lifetime of the droplet decreases and is in general agreements with experimental and modelling results [34,10,22]. Further, it was observed that as Re_g is decreased, the evaporation lifetime increased in the same manner with respect to the pressure. Also the evaporation follows the d^2-*law*.

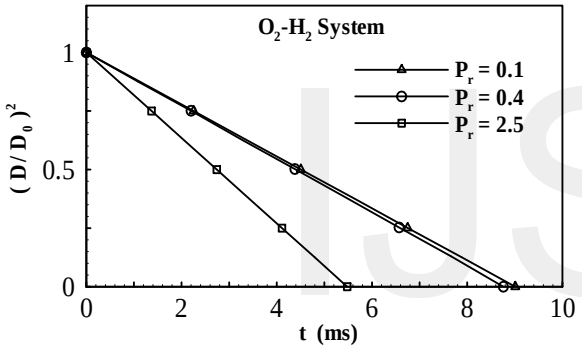

Figure 10: Square of dimensionless droplet diameter versus time for Re_g = 100

3.7 Droplet Evaporation Rate Versus Time at Different Ambient Pressures for a Fixed Value of Reynolds Number and Ambient Temperature

A plot of m_{ev} with time for a $100\,\mu m$ diameter oxygen droplet vaporising in hydrogen atmosphere at P_r =0.1, 0.4 and 2.5 and T_∞ =1000 K is depicted in Fig 11. It is observed that the evaporation rate was highest in the beginning and gradually reduced to a minimum value at the end of the droplet lifetime for each pressure. The m_{ev} versus time plot were quite similar for P_r =0.1 and 0.4, but there was a sudden increase in evaporation rate for the supercritical pressure corresponding to P_r = 2.5, as a result the droplet gets consumed in about 5.5 ms. However, as Re_g is reduced, m_{ev} reduces thereby increasing the droplet lifetime.

3.8 Droplet Diameter Effect on Lifetime and Burning Rate

For investigating this effect, the droplet size was varied from 20 to 2000 microns. From Figs 12-13, it was observed that for a particular droplet

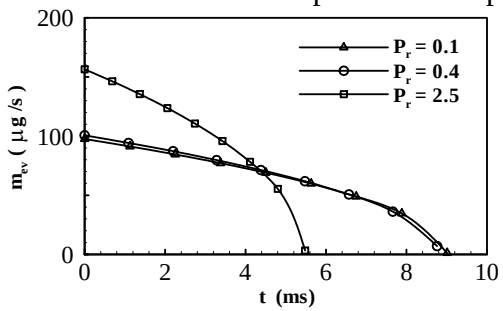

Figure 11: Vaporisation rate at different times for Re_g = 100

diameter, an increase in pressure decreased the droplet lifetime, whereas burning rate was enhanced. Also, lifetime and burning rate increased as droplet size was increased at a given pressure.

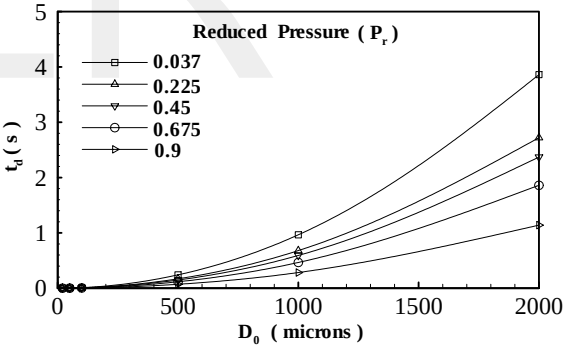

Figure 12: Effect of variation of initial droplet diameter D_0 on droplet lifetime t_d at a fixed value of P_r for n - heptane (T_∞ = 298 K, $Y_{o,\infty}$ = 0.232)

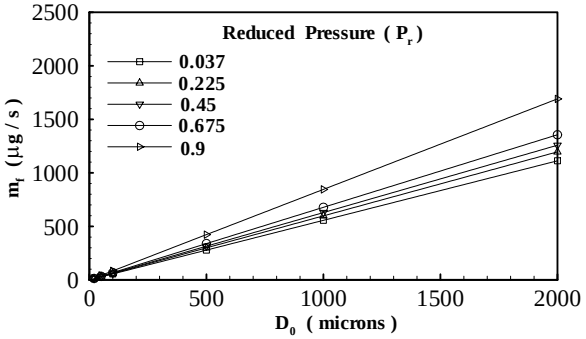

Figure 13: Droplet mass burning rate

3.9 Droplet Size Effect on Other Burning Characteristics

The present code was used for a wide range of initial or original droplet diameter D_0 ranging from 20 to 5000 microns covering three important burning regimes namely homogeneous $D_0 \leq 20$ microns, transition $30 \leq D_0 \leq 80$ microns and heterogeneous $D_0 > 80$ microns.

It was observed from Figs (14–15) for a n-heptane droplet undergoing combustion in standard atmosphere that when the variation of flame diameter F (determined from computed results) was plotted against dimensionless time t/t_d, flame diameter first increased, reached a maxima and then decreased towards the end of the droplet lifetime. This behaviour is consistent with the transient burning of the droplet verified by experiments. It was further noted that for $D_0 > 50$ microns, there was a gradual increase in value of flame diameters, being about 0.375 cm and 4 cm for 500 and 5000 micron droplet respectively. For $D_0 \leq 50$ microns, the increase in flame diameters F with D_0 was small. It was also observed that the maximum value of flame diameter F occured when about 25% of droplet burning was completed ($t/t_d \approx 0.25$).

From above results, it can be said that for a particular fuel, as the droplet size increased, its surface area increased correspondingly which gave rise to increased evaporation rate of fuel vapour from the droplet surface and hence bigger flame diameters.

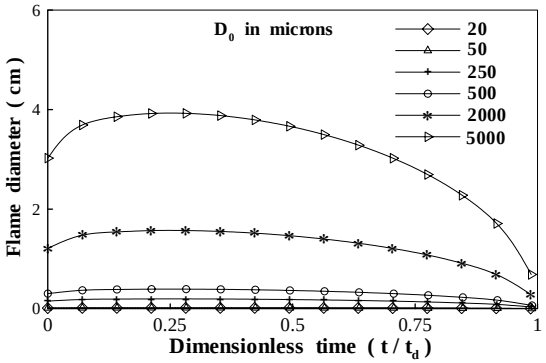

Figure 14: Variation of flame diameter F with dimensionless time t / t_d for different initial droplet sizes of n-heptane (P_∞ = 1 atm, T_∞ = 298 K, $Y_{o,\infty}$ = 0.232)

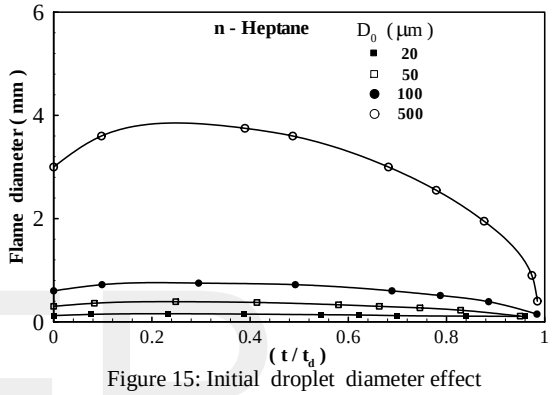

Figure 15: Initial droplet diameter effect

It could be inferred from Fig 16 that for a n-heptane droplet burning in standard conditions, there was a linear variation of $(D/D_0)^2$ with time. It was further observed that as the droplet size was increased from 20 to 500 microns, there was a corresponding increase in droplet lifetime.

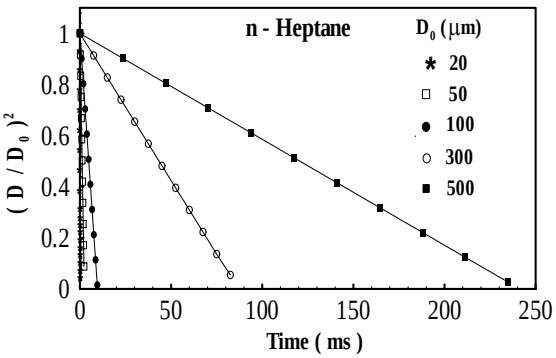

Figure 16: Square of dimensionless droplet diameter versus time

From Figure 17, it was observed that for a given fuel, an increase in the droplet size led to an increase in the flame standoff distance. It was also noted that the

flame standoff distance first increased, reached a maxima and then decreased, emphasising that droplet combustion is an unsteady phenomenon as verified by experiments.

4 CONCLUSIONS

The present model provides the necessary information regarding droplet vaporisation at high

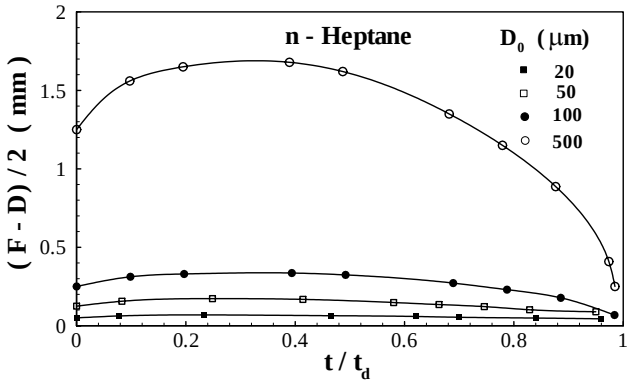

Figure 17: Flame standoff distance variation with time

pressures which includes pressure effects on burning constant, burning rate and droplet lifetime (in non convective and convective environments), variation of critical mixing temperature, solubility of ambient gas in the liquid, variation of vapour mass fraction with droplet temperature at various pressures and vaporisation behaviour in hot convective surrounding at different pressures. The predictions of the present study were in good agreement when compared with the experimental data and theoretical results of other authors who have used more complicated models.

Feeling the need to explore the effect of initial droplet size on burning, a spherically symmetric, transient gas phase droplet combustion model was evolved and the effects of initial droplet diameter on important droplet burning parameters were quantified. Further, the versatility code was tested by handling a wide range of droplet diameters ranging from 20 to 5000 microns (0.02mm-5mm). The gas phase model of the present work can be further investigated with respect to ambient temperature, composition and different fuels.

TABLE 1
Summary of Important Equations of State and their Constants.

Equation	u	ω	b	a
Van der Waals	0	0	$\frac{R_u T_c}{8P_c}$	$\frac{27}{64}\frac{R_u^2 T_c^2}{P_c}$
Redlich- Kwong	1	0	$\frac{0.08664 R_u T_c}{P_c}$	$\frac{0.42748 R_u^2 T_c^{2.5}}{P_c T^{0.5}}$
Soave-Redlich-Kwong	1	0	$\frac{0.08664 R_u T_c}{P_c}$	$\frac{0.42748 R_u^2 T_c^2}{P_c}\left[1+f(\omega)\left(1-T_r^{0.5}\right)\right]^2$ where, $f(\omega)=0.48+1.574\omega-0.176\omega^2$
Peng-Robinson	2	-1	$\frac{0.07780 R_u T_c}{P_c}$	$\frac{0.42748 R_u^2 T_c^2}{P_c}\left[1+f(\omega)\left(1-T_r^{0.5}\right)\right]^2$ where, $f(\omega)=0.37464+1.5423\omega-0.26992\omega^2$

TABLE 2
Effect of Ambient Pressure on k_b, t_d and m_f for n-Heptane
($D_0 = 2000\mu m$)

Reduced Pressure $P_r = P_\infty / P_c$	**Ambient Pressure** P_∞ (atm)	**Burning Constant** k_b (mm^2/s)	**Droplet Lifetime** t_d (s)	**Mass Burning Rate** m_f (mg/s)
0.037	1.0	1.036	3.86	1.113
0.225	6.075	1.47	2.72	1.196
0.450	12.15	1.69	2.37	1.258
0.675	18.225	2.15	1.86	1.356
0.900	24.3	3.53	1.14	1.691

REFERENCES

[1] W. A. Sirignano "Fluid Dynamics and Transport of Droplets and Sprays", Cambridge University Press, 1999.

[2] K. Harstad and J. Bellan, "Evaluation of Commonly Used Assumptions for Isolated and Cluster Heptane Drops in Nitrogen at All Pressures", Combustion and Flame, Vol. 127, pp. 1861-1879, 2001.

[3] D. B. Spalding, "Theory of Particle Combustion at High Pressure", ARS J, 29, pp. 828-835, 1959.

[4] D. E. Rosner, "On Liquid Droplet Combustion at High Pressures", AIAA Journal,Vol. 5, pp. 163-166,1967.

[5] T. A. Brzustowski, "Chemical and Physical Limits on Vapour Phase Diffusion Flames of Droplets", Canadian J. Chem. Engr, 43, pp. 30-36, 1965.

[6] J. A. Manrique and G. L. Borman, "Calculations of Steady State Droplet Vaporization at High Ambient Pressure", Int. J. Heat Mass Transfer, Vol. 2, pp. 1081-1095, 1969.

[7] R. S. Lazar and G. M. Faeth, "Bipropellant Droplet Combustion in the Vicinity of the Critical Point", Proceedings of the Thirteenth

Symposium (International) on Combustion, The Combustion Institute, pp. 801-811, 1971.

[8] G. S. Canada and G. M. Faeth, "Combustion of Liquid Fuels in a Flowing Combustion Gas Environment at High Pressures", Proceedings of the Fifteenth Symposium (International) on Combustion, The Combustion Institute, pp. 418-428, 1975.

[9] D. E. Rosner and W. S. Chang, "Transient Evaporation and Combustion of a Fuel Droplet Near its Critical Temperature", Combustion Science and Technology, Vol. 7, pp. 145-158, 1973.

[10] T. Kadota and H. Hiroyasu, H.,"Combustion of a Fuel Droplet in Supercritical Gaseous Environments", Proceedings of the Eighteenth Symposium (International) on Combustion, The Combustion Institute, pp. 275-282, 1981.

[11] J. S. Chin and A. H. Lefebvre, "Steady-State Evaporation Characteristics of Hydrocarbon Fuel Drops", AIAA Journal, Vol. 21, No.10, pp.1437-1443, 1983.

[12] K. C. Hsieh, J. S. Shuen and V. Yang, "Droplet Vaporization in High Pressure Environments 1: Near Critical Conditions", Combustion Science and Technology, Vol. 76, pp. 111-132, 1991.

[13] E. W. Curtis and P. V. Farrell, "A Numerical Study of High Pressure Droplet Vaporization", Combustion and Flame, Vol. 90, pp. 85-102, 1992.

[14] H. Jia and G. Gogos, "Investigation of Liquid Droplet Evaporation in Subcritical and Supercritical Gaseous Environments", J. Thermophys. Heat Transfer, 6, pp. 738-745, 1992.

[15] J. P. Delplanque and W. A. Sirignano, "Numerical Study of the Transient Vaporization of an Oxygen Droplet at Sub and Supercritical Conditions" Int. J. Heat Mass Transfer, Vol. 36, pp. 303-314, 1993.

[16] K. Harstad and J. Bellan, "Isolated Fluid Oxygen Drop Behaviour in Fluid Hydrogen at Rocket Chamber Pressures", Int. J. Heat Mass Transfer, Vol. 41, pp. 3537-3550, 1998.

[17] K. Harstad and J. Bellan, "Interactions of Fluid Oxygen Drops in Fluid Hydrogen at Rocket Chamber Pressures", Int. J. Heat Mass Transfer, Vol. 41, pp. 3551-3558, 1998.

[18] K. Harstad and J. Bellan, J., "The Lewis Number Under Supercritical Conditions", Int. J. Heat Mass Transfer, Vol. 42, pp. 961-970, 1999.

[19] K. Harstad and J. Bellan, "An All Pressure Fuel Drop Model Applied to a Binary Mixture: Heptane in Nitrogen", Intl. J. Multiphase Flow, 26, pp. 1675-1706, 2000.

[20] A. Umemura and Y. Shimada, "Characteristics of Supercritical Droplet Gasification", Twenty Sixth Symposium (International) on Combustion, The Combustion Institute, pp. 1621-1628, 1996.

[21] G. Zhu, and S. K. Aggarwal, "Transient Supercritical Droplet Evaporation with Emphasis on the Effects of Equation of State", Int. J. Heat Mass Transfer, Vol. 43, pp. 1157-1171, 2000.

[22] V. Yang, "Modelling of Supercritical Vaporization, Mixing and Combustion Processes in Liquid Fueled Propulsion Systems", Proceedings of the Twenty Eighth Symposium (International) on Combustion, The Combustion Institute, pp. 925-942, 2000.

[23] B. Vieille, C. Chauveau, X. Chesneau, A. Odeïde and I. Gökalp, "High Pressure Droplet Burning Experiments in Microgravity", Proceedings of the Twenty Sixth Symposium (International) on Combustion, The Combustion Institute, pp. 1259-1265, 1996.

[24] J. Stengele, K. Prommersberger, M. Willmann and S. Wittig, "Experimental and Theoretical Study of One and Two Component Droplet Vaporization in a High Pressure Environment", Int. J. Heat Mass Transfer, Vol. 42, pp. 2683-2694, 1999.

[25] Hongsuk. Kim and Nakwon. Sung, "The effect of Ambient Pressure on the Evaporation of a Single Droplet and a Spray", Combustion and Flame, Vol.135, pp. 261-270, 2003.

[26] C. K. Law, "Recent Advances in Droplet Vaporization and Combustion", Progress in Energy and Combustion Science, Vol. 8, pp. 171-201, 1982.

[27] S. Kumagai, and H. Isoda, "Combustion of Fuel Droplets in a Falling Chamber", Proceedings of the Sixth Symposium (International) on Combustion, Reinhold, N.Y., pp. 726-731, 1957.

[28] C. K. Law and G. M. Faeth, "Opportunities and Challenges of Combustion in Microgravity", Progress in Energy and Combustion Science, Vol. 20, pp. 65-113, 1994.

[29] C. H. Waldman, "Theory of Non-Steady State Droplet Combustion", Fifteenth Symposium (International) on Combustion, The Combustion Institute, pp. 429-442, 1974.

[30] S. Ulzama and E. Specht, "An Analytical Study of Droplet Combustion Under Microgravity: Quasi-Steady Transient Approach", Proceedings of the Thirty First Symposium (International) on Combustion, The Combustion Institute, pp. 2301-2308, 2007.

[31] I. K. Puri and P. A. Libby, "The Influence of Transport Properties on Droplet Burning", Combustion Science and Technology, Vol. 76, pp. 67-80, 1991.

[32] M. K. King, "An Unsteady-State Analysis of Porous Sphere and Droplet Fuel Combustion Under Microgravity Conditions", Proceedings of the Twenty Sixth Symposium (International) on Combustion, The Combustion Institute, pp.1227-1234, 1996.

[33] R. C. Reid, J. M. Prausnitz, and B. E. Poling, "The Properties of Gases and Liquids", Fourth Edition, McGraw Hill Book Company, 1989.

[34] K. K. Kuo, "Principles of Combustion", Second Edition, John Wiley and Sons, 2005.

[35] M. K. Jain, "Numerical Solution of Differential Equations", Second Edition, Wiley-Eastern Limited, 1984.

[36] O. L. Gülder, "Flame Temperature Estimation of Conventional and Future Jet Fuels", Transactions of the ASME, Vol. 108, pp. 376-380, 1986.

[37] H. Nomura, Y. Ujiie, H. J. Rath, J. Sato, and M. Kono, "Experimental Study on High Pressure Droplet Evaporation Using Microgravity Conditions", Proceedings of the Twenty Sixth Symposium (International) on Combustion, The Combustion Institute, pp. 1267-1273, 1996.

[38] Faeth et al., "Supercritical Bipropellant Droplet Combustion", Proceedings of the Twelfth International Symposium on Combustion, The Combustion Institute, pp. 9-17, 1969.

[39] H. Jia and H. Gogos, "High Pressure Droplet Vaporization; Effects of Liquid-Phase Gas Solubility", International Journal of Heat and Mass Transfer, Vol. 26, No.18, pp. 4419-4431, 1995.

[40] S. Kotake and T. Okazaki, "Evaporation and Combustion of a Fuel Droplet", Int. J. Heat Mass Transfer, Vol. 12, pp. 595-609, 1969.

[41] A. H. Lefebvre, "Atomization and Sprays", Hemisphere Publishing Corporation, Philadelphia, London, 1989.